MAGNETIC RESONANCE IN CHEMISTRY, VOL. 36, 415–421 (1998)

High-Resolution Solid-State Nuclear Magnetic Resonance Study of the Tetrapropylammonium Template in a Purely Siliceous MFI-Type Zeolite

R. Gougeon,[1]† L. Delmotte,[1] P. Reinheimer,[2] B. Meurer[3] and J. M. Chézeau[1]*

[1] Ecole Nationale Supérieure de Chimie de Mulhouse, 3 Rue Alfred Werner, F-68093 Mulhouse cedex, France
[2] Université Louis Pasteur, Institut Lebel, Laboratoire RM3, 4 Rue Blaise Pascal, F-67008 Strasbourg Cedex, France
[3] Institut Charles Sadron, 6 Rue Boussingault, F-67083 Strasbourg cedex, France

Received 9 June 1997; revised 19 January 1998; accepted 19 January 1998

ABSTRACT: The dynamics of tetrapropylammonium (TPA) cations occluded during the synthesis of a siliceous MFI zeolite were investigated by several ^{13}C high-resolution NMR methods. This work follows and complements a previous ^{1}H broad-line NMR study of this material. The evolution of the ^{13}C cross polarization magic angle spinning (CP/MAS) spectrum of the template inside the structure was studied over a wide temperature range, from 120 to 463 K. Through the indirect measurements of ^{1}H dipolar couplings via ^{13}C CP/MAS NMR, it is possible to differentiate one of the carbons linked to nitrogen from the others, in terms of hindrance to motion. A high-frequency oscillation of the entire cation is superimposed, as shown by ^{13}C T_1 measurements. This study confirmed the great mobility of the template already observed by ^{1}H broad-line measurements and also revealed that this mobility increases on going from the inner to the outer part of the propyl arms. © 1998 John Wiley & Sons, Ltd.

KEYWORDS: NMR; ^{13}C cross-polarization magic angle spinning NMR; solid-state dynamics; tetrapropylammonium template; siliceous MFI zeolite

INTRODUCTION

The use of organic molecules as templates, first introduced in zeolite synthesis by Barrer and Denny,[1] is responsible for the synthesis of a number of new structures[2] and also for the extension of the range of framework compositions, especially towards high Si/Al ratios.[3] For example, purely siliceous MFI-type zeolite has not yet been obtained without a template.[4] During the synthesis, the organic species are trapped in the framework and can only be removed by thermal decomposition. A high residual mobility of the template inside the framework seems fairly frequent, however,[5] but up to now very little quantitative information has appeared on the detailed nature and dynamics of these motions.[6,7] The quantitative study of these geometrically highly constrained motions should prove interesting as a test for theoretical anisotropic correlation functions. Moreover, it would permit the investigation of the interaction between the template and the framework in order to devise more accurate interatomic potentials for such compounds, which in turn would allow a better understanding of the role of the template during the crystallization. Although molecular modelling proved to be useful in synthesis design, it has been of very limited success in zeolite synthesis. So far, it has not been possible to predict which new structure would be obtained from a given template, or which new template should be used to obtain a known structure. The only noticeable exception was the selection of tris(2-trimethylaminoethyl)amine as a suitable template for ZSM-18.[8]

In a previous paper,[9] referred to in the following as Part 1, and dealing with ^{1}H broad-line NMR measurements (second moments, relaxation times T_1 and $T_{1\rho}$), the mobility of tetrapropylammonium cation (TPA) in a purely siliceous MFI framework was compared with that of the same entity in pure bulk tetrapropylammonium bromide (TPABr). This study revealed the higher mobility of the template inside the framework from 100 to 378 K, the temperature of a phase transition in TPABr. However, the framework prevents the quasi-isotropic molecular tumbling from occurring in the zeolite. This study also revealed the complexity of the motions of the template, which could not be accounted for by simple models. Since the four propyl arms are each engaged in a different channel, they should exhibit different motions. Numerous studies described in the literature have demonstrated the power of ^{13}C magic angle spinning (MAS) and cross-polarization (CP) MAS techniques for investigating local dynamics in polymers[10] or more general molecular dynamic phenomena in the solid state.[6,7,11–14] This paper reports a combination of ^{13}C high-resolution CP/MAS techniques in order to obtain more detailed information on the motion of the TPA cation occluded in the purely siliceous MFI-type zeolite.

* *Correspondence to*: J. M. Chézeau, Ecole Nationale Supérieure de Chimie de Mulhouse, 3 Rue Alfred Werner, F-68093 Mulhouse cedex, France.
† Present address: Department of Chemistry, University of Durham, Durham DH1 3LE, UK.

 CCC 0749-1581/98/060415–07 $17.50

EXPERIMENTAL

The siliceous MFI zeolite was prepared in a fluoride-containing medium by hydrothermal synthesis at 200 °C. The sample was the same as in Part 1,[9] where more details concerning the synthesis and the characterization can be found.

Except for the high-temperature CP/MAS spectra, all the ^{13}C NMR measurements were conducted on a Bruker MSL 300 spectrometer at 75.470 MHz, using a 7 mm o.d. Bruker double-bearing MAS probe. The high-temperature CP/MAS spectra were acquired on a Bruker DSX 300 spectrometer operating at 75.41 MHz, using a 4 mm o.d. Bruker double-bearing probe. ^{13}C chemical shifts were referenced relative to the CH_2 group in adamantane at 38.56 ppm. All the ^{1}H–^{13}C CP/MAS spectra were obtained by cross-polarization, with proton dipolar decoupling (DD). The spin-locking radiofrequency fields for both carbon and hydrogen were 54 or 75 kHz (high-temperature spectra).

All the spectral processing was performed using Bruker WIN-NMR and WINFIT software and the mathematical treatments using MATHEMATICA software (Wolfram Research).

Variable-temperature ^{13}C CP/MAS study

^{13}C CP/MAS spectra were recorded as a function of temperature from 120 to 473 K. For this study, and for low temperatures, the zirconia rotor was fitted with a special PTFE cap, which allowed a spinning speed of about 3.5 kHz down to 120 K. After each temperature change, the sample was allowed to equilibrate for at least 15 min. The presence of a small quantity of adamantane in the rotor during variable-temperature measurements permitted us to follow the variation of chemical shifts with decreasing temperature and to evaluate an uncertainty of about 3 K in the temperature measurements. The repetition times varied from 5 to 30 s according to variable-temperature ^{1}H T_1 measurements in Part 1.[9] The contact times are indicated on the figures.

^{1}H dipolar local field measurements

In order to investigate the local mobility through the study of H–H dipolar coupling, the cross-polarization modified experiment initially proposed by Tekely *et al.*[15] was used. In this experiment (Fig. 1), after a 90° pulse, the proton magnetization is allowed to dephase under the H–H dipolar interaction for a variable delay, followed by the polarization transfer. Palmas *et al.*[16] showed that for strong ^{1}H–^{13}C couplings, in addition to proton dipolar coupling, this experiment could reflect ^{1}H–^{13}C coupling and even be mainly dependent on the latter. Consequently, and in order to observe only proton dipolar coupling, ^{13}C dipolar decoupling was applied during the evolution time τ.[16] In that case, for a

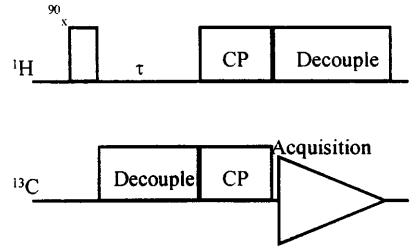

Figure 1. Pulse sequence used for indirect ^{1}H–^{1}H dipolar local field measurements through high-resolution ^{13}C CP/MAS NMR.[16]

sufficiently short contact time to avoid spin diffusion and with increasing τ, each ^{13}C peak of the CP/MAS spectrum should decrease in a characteristic time equal to the spin–spin relaxation time $T_2(^{1}H)$ of the protons bonded to the corresponding carbon.[16] The contact time was 50 μs and the CP/MAS spectrum was recorded for 128 incremented values of τ. The Hartmann–Hahn conditions were the same as above (r.f. field 54 kHz). ^{1}H second moments (M_2) associated with each ^{13}C resolved line can be derived from the relaxation times $T_2(^{1}H)$ using the following approximations, wherever appropriate: Gaussian decrease; $M_2 = 1/T_2^2$, or Pake decrease, $M_2 = b^2 + 1/T_2^2$, where b accounts for an oscillation of the FID due to a dominant contribution of an isolated spin pair. The uncertainty in T_2 is <1 μs.

The ^{1}H MAS spectrum was recorded at room temperature at a frequency of 300 MHz and a spinning speed of 12 kHz. The ^{1}H CRAMPS spectrum of the zeolite sample was recorded at room temperature and a frequency of 298.7 MHz using the BR-24 sequence. The spinning speed was 2 kHz and the pulse duration 1.8 μs. For both ^{1}H spectra, the repetition time was 5 s.

^{13}C T_1 measurements

For each line of the different carbons, ^{13}C T_1 measurements were performed over the temperature range 253–353 K, using the Torchia sequence,[17] with contact times between 1 and 10 ms. They were also recorded with the standard inversion–recovery ^{13}C single pulse experiment at room temperature (298 K). The ^{13}C 90° pulse was 4.5 μs and the relaxation delay was 5 s.

RESULTS AND DISCUSSION

Variable-temperature CP/MAS study

The ^{13}C CP/MAS spectra of TPA enclosed in the zeolite framework are displayed in Figs 2 and 3 at temperatures ranging from 120 to 463 K. At the lowest temperature, each signal arising from a distinct carbon along the alkyl chain (denoted in the following as C-1, C-2 and C-3, starting from the carbon linked to nitrogen) exhibits several peaks. We will label the peaks with letters (A–L) in the low-temperature monoclinic

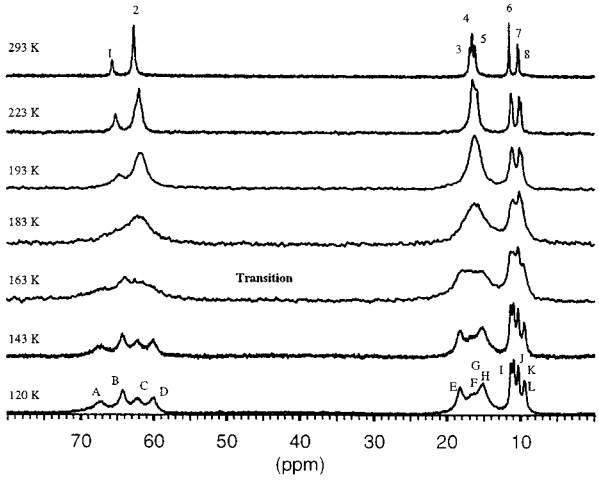

Figure 2. ^{13}C CP/MAS spectra of the as-synthesized siliceous MFI-type zeolite at several temperatures ranging from 120 to 293 K. Contact time $\tau_{CP} = 100$ μs (120 μs at 293 K), spinning speed $\nu_{rot} = 3.6$ kHz and number of transients $N_s = 64$ (128 at 293 K).

phase and with numbers (1–8) in the orthorhombic phase. In the monoclinic phase, four peaks can clearly be distinguished for the C-1 and C-3 signals, whereas at least three components are seen on the C-2 signal. The separation between the extreme peaks belonging to the same carbon signal varies from 535 Hz for C-1 to 142 Hz for C-3. These spectra do not change much from 120 to 143 K. At 163 K, a general broadening of all the individual peaks occurs, without a noticeable change in the position of these peaks. The shape of each of the carbon signals is reminiscent of the envelope of the better resolved signals observed at lower temperatures.

More important changes are brought about by the phase transition from the monoclinic to the orthorhombic structure, which was detected in the vicinity of 175 K by both thermal analysis and x-ray powder diffraction pattern studies.[18] However, a variable-temperature ^{29}Si MAS NMR study revealed only a very progressive change.[18] At 183 K, a temperature at which all the signals are broad, the spectrum already exhibits the general features of the much better resolved one at room temperature. The maximum of the C-1 signal has shifted to a lower frequency, with a shoulder on its high-frequency side. With increasing temperature, this shoulder evolves into a new peak eventually observed at 65.65 ppm at room temperature. A similar evolution is shown by the C-3 signal. At 183 K, the two higher frequency peaks observed at lower temperatures merge into only one, the width of which subsequently decreases with increasing temperature. A very narrow splitting of the lower frequency component is also observed at 223 K and above. The narrowing of the C-2 signal between 183 and 293 K is also clear. Starting from a broad, featureless signal at 183 K, it is only at room temperature that three very close and narrow components can clearly be distinguished.

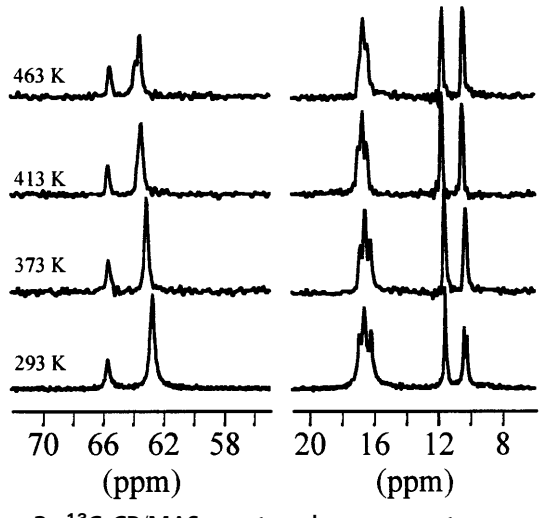

Figure 3. ^{13}C CP/MAS spectra above room temperature. $\tau_{CP} = 1$ ms, $\nu_{rot} = 5$ kHz and $N_s = 64$. The C-1 and C-2, C-3 peak regions are magnified for a better view.

Above room temperature, the lowest frequency peak of the C-1 signal surprisingly splits into two components, clearly visible at 463 K. On the other hand, both lowest frequency peaks of the C-3 signals merge into one peak at 373 K (Fig. 3). With increasing temperature, the C-2 signal regularly narrows.

The small linewidth of the four C-3 peaks, in the monoclinic phase, is related to a rapid reorientation of methyl groups already observed at very low temperature.[9] These multiple lines consequently show a picture of the distinct environments surrounding each arm of a TPA cation, associated with very good crystallinity of the sample. In the case of the C-1 carbons, multiple lines can arise from quadrupolar coupling with nitrogen.[19] However, two arguments may be advanced against this hypothesis: first, we checked that areas under the C-1 peaks, 1:1:1:1, were different from the 2:1 doublet pattern expected,[19] and second, no variation of the C-1 peaks in the temperature range 120–143 K could be observed (Fig. 2), though quadrupolar coupling with ^{14}N is strongly temperature dependent.[20] Consequently, both the good crystallinity and the slow motion of at least the C-2 and C-3 carbons, of the order of 300 kHz at about 160 K,[9] can account for the resolution of multiple lines for the different carbons at very low temperatures.

The CP/MAS spectrum exhibits at 163 K an overall broadening of the peaks (Figs 2 and 4). ^{29}Si MAS NMR spectra of this zeolite recorded at temperatures around the phase transition (175 K) also exhibit an overall line broadening of the peaks.[18] These observations can be explained by the fact that the phase transition takes place progressively below and above 175 K or in an inhomogeneous way throughout the sample. The ^{29}Si and ^{13}C spectra should consequently reflect the existence of both phases in the sample, over a 10–20 °C wide temperature range.

The difference between the CP/MAS spectrum at 183 K and that at 163 K clearly indicates that the phase transition not only acts on the low-frequency motion of the cation[9] but also modifies the conformational structure of the cation. The spectrum at 183 K already

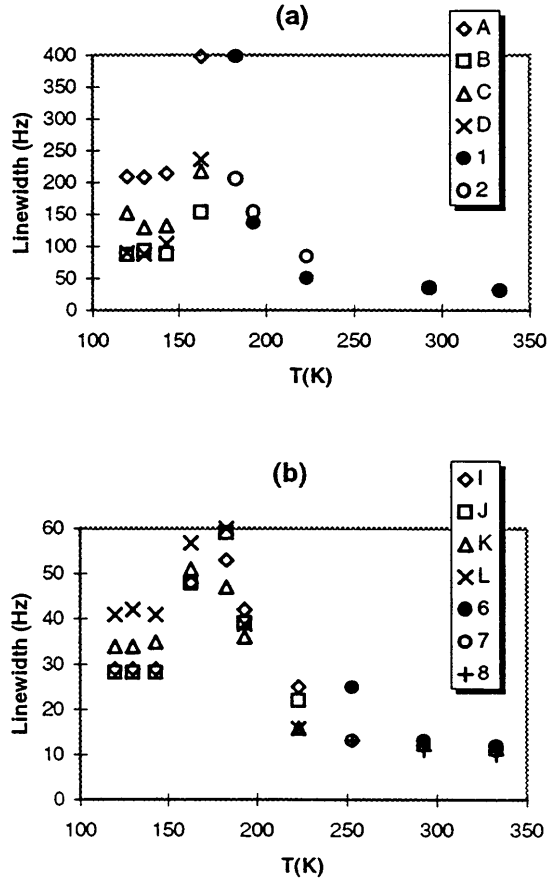

Figure 4. Linewidth at half-height for each of the ^{13}C signals (C-1 and C-3) as a function of temperature: (a) C-1; (b) C-3. The detailed attribution of the peaks is given in the inserts, and is the same as in Fig. 2.

exhibits the shape of the better resolved spectrum at ambient temperature. However, careful deconvolution of the spectra on both sides of the transition allows us to connect reasonably some of the peaks of each phase through the evolution of both peak widths and chemical shifts. For example, Fig. 4 shows the evolution with temperature of the peak widths for the C-1 and C-3 carbons. For the former, peak A shows the highest linewidth below the transition. On the other side of the transition, peak 1 exhibits the broadest linewidth. Consequently, these two peaks can probably be assigned to the same carbon linked to nitrogen. Peaks B, C and D merge into peak 2 of the orthorhombic phase. Owing to the broad, featureless signal of the C-2 carbons immediately above the transition, no such correspondence can be obtained for these peaks. Eventually, due to the fast motion of the methyl groups, we can more easily follow the C-3 peaks through the transition. We can distinguish peaks I, J, K and L up to 223 K, where I and J merge into peak 6. This continuity through the transition agrees with the study of relaxation times reported in Part 1.[9] The H T_1 values, which are mainly controlled by the methyl group rotation in this temperature range, are not disturbed by the transition. On the other hand, $T_{1\rho}$ values, which reflect slow motions, mainly involving the protons of C-1 and C-2 carbons, undergo a discontinuity.

At room temperature, in the orthorhombic phase, all the peaks are very narrow, indicating a strong motional narrowing, in agreement with the ^1H second moment measurements reported in Part 1.[9] The deconvolution of the ^{13}C MAS dipolar decoupled spectrum at room temperature (not shown) leads to relative intensities for peaks 1–8 of 1:3:1:2:1:2:1:1. It has already been shown that the doublet pattern of the C-1 peaks does not arise from nitrogen quadrupolar coupling,[21] One explanation for the reduction in the number of distinct peaks with increasing temperature through the transition could be the gain in symmetry. Some of the carbons inequivalent in the monoclinic phase may become equivalent in the orthorhombic phase.

Figure 3 shows the magnified high-temperature ^{13}C CP/MAS spectra of the zeolite. Whereas the C-2 and C-3 peaks evolve into a logical motional narrowing and merge with increasing temperature, peak 2 of the C-1 carbons splits into two resolved peaks at 463 K. This may be associated with the observed ^1H $T_{1\rho}$ decrease in this temperature domain, reported in Part 1,[9] which reveals a supplementary, unidentified, slow motion.

Dipolar local field measurements from indirect observation of ^1H nuclei

The motional averaging of the ^1H–^{13}C dipolar coupling is one of the most relevant effects for the investigation of the local dynamics of aliphatic units.[10] However, mainly owing to spin diffusion, it is difficult to take advantage of the simple cross-polarization experiment.[22] We chose to investigate the carbon mobility of the TPA cation at ambient temperature, through measurements of H–H dipolar coupling as described above. A contact time of 50 μs was taken as short enough for the spin diffusion to be inefficient. As an example, Fig. 5 exhibits the decrease in the intensity of peaks 2 and 8 in the CP/MAS spectrum at ambient temperature as a function of the length of the H–H dephasing delay. Owing to the lack of resolution, peaks 3, 4 and 5 were treated globally. The decreases of peaks 1 and 2 were fitted to the sum of a Gaussian curve and a Pake curve[23] to account for the oscillation. The decrease of peaks 3 + 4 + 5 was fitted to a Gaussian curve and those of peaks 6, 7 and 8 were fitted to an exponential curve. The characteristic times and corresponding second moments are given in Table 1. The decrease of peak 2 exhibits a more pronounced oscillation than that of peak 1 (not shown in Fig. 5). This oscillation, which is not observed for peaks 3 + 4 + 5, reflects that the two protons of the C-1 carbon constitute a well isolated spin pair, but also the hindrance of the rotational motion of this pair around N—C bonds. Indeed, the major contribution, which is that of the Gaussian curve, has a characteristic time of 12.8 and 12 μs (±0.5 μs) for peaks 1 and 2, respectively, whereas for a rigid H–H doublet this calculated characteristic time is 11.1 μs. It can be concluded that the carbon corresponding to peak 1 exhibits greater mobility than that associated

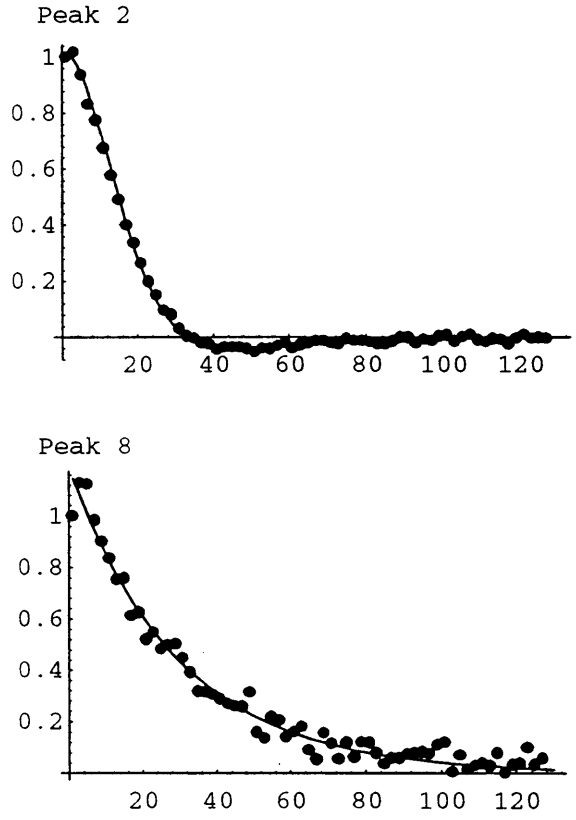

Figure 5. ^{13}C signal decays as a function of the evolution time before the magnetization transfer (pulse sequence of Fig. 1) τ_{CP} is constant (50 μs). The fitting curves are those described in Table 1. The values on the ordinate are in arbitrary units and those on the abscissa are in μs. Only peaks 2 and 8 are presented.

with peak 2. Furthermore, this mobility increases on going from nitrogen to methyl groups. The exponential decrease of the methyl signals agrees with the high rotational mobility of these groups. However, it can be inferred from Table 1 that the methyl group corresponding to peak 8 has greater mobility than the others. It must be pointed out that second moments calculated from these experiments (Table 1) are in good agreement with the value obtained experimentally in Part 1,[9] i.e. 4.7 G^2 at ambient temperature. Indeed, if we consider that the second moments of methyl groups are negligible owing to fast motion, the global value obtained from this experiment, using the second moments in Table 1, is 4.4 G^2.

The M_2 values in Table 1 are related to CH_2 groups. Consequently, the difference of 0.3 G^2 between the two values should be attributed to either an inter-CH_3 group contribution or to a weak contribution of methyl groups to the second moment.

By Fourier transformation of these proton free induction decays, ^1H dipolar spectra corresponding to each ^{13}C-resolved peak are obtained (Fig. 6). The oscillatory character of the decrease of peaks 1 and 2 hence appears as a Pake doublet shape in the corresponding spectrum. The comparison of these dipolar spectra with either the ^1H CRAMPS spectrum or the high-resolution MAS (12 kHz) spectrum of the zeolite sample (Fig. 6) is interesting. The very narrow lines of the CRAMPS spectrum (*ca.* 60 Hz) compared with those of the dipolar spectra (*ca.* 30 kHz for C-1 and C-2 carbons and 15 kHz for methyls) clearly indicate the strong H–H homonuclear coupling of the TPA cation. This coupling is not averaged either by the macroscopic rotation or by the high local dynamics of the cation,[9] but is efficiently eliminated by the CRAMPS technique. Despite rapid internal rotation, even the dipolar spectra of methyl groups remain fairly broad. This could indicate important molecular packing effects and specific organic-framework interactions.

^{13}C T_1 study

Figure 7 shows the variation with temperature of ^{13}C T_1 values for each resolved peak of the CP/MAS spectrum. The temperature range extends from 253 to 353 K. Our values clearly differ from those of Cheng *et al.*[20]

Table 1. ^1H local field parameters obtained by analysis of each ^{13}C signal decay as those shown in Fig. 5[a]

	Gaussian curve		Pake curve			
			Gaussian			
Peak	%	T_2 (μs)	%	T_2 (μs)	Oscillation period (μs)	Second moment, M_2 (G^2)
1	81	12.8	18	26	157	8.2
2	83	12	17	30	121	9.1

Peak	Gaussian curve, T_2 (μs)	Exponential curve, T_2 (μs)	Second moment (G^2)
3 + 4 + 5	14.3		6.8
6		22.2	
7		26.7	
8		29.9	

[a] The derivation of the second moment is described in the experimental section.

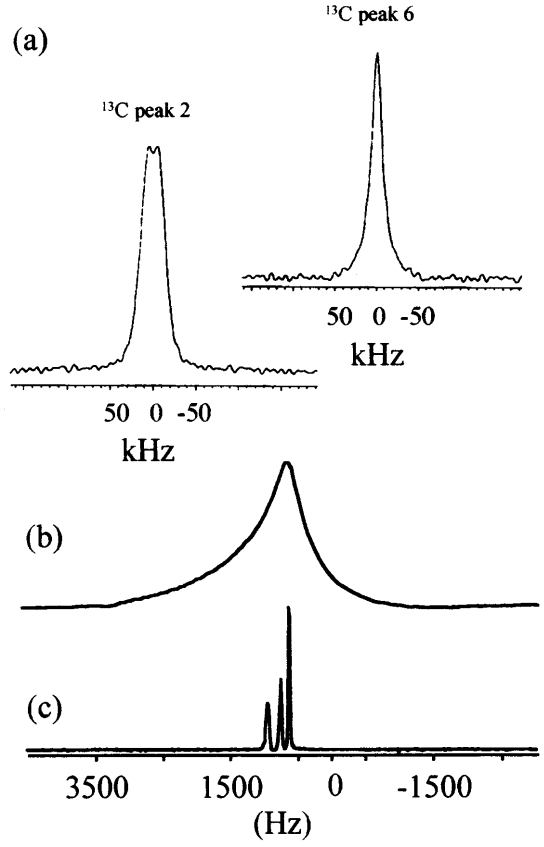

Figure 6. ^{1}H spectra of the as-synthesized siliceous MFI-type zeolite: (a) reconstructed dipolar spectra associated with peaks 2 and 6 of the ^{13}C spectrum, by Fourier transformation of the FIDs; (b) MAS spectrum, $\nu_{rot} = 12$ kHz, $D_0 = 5$ s; (c) CRAMPS spectrum using the BR-24 pulse sequence, $\nu_{rot} = 2$ kHz, pulse duration = 1.8 μs and $D_0 = 5$ s.

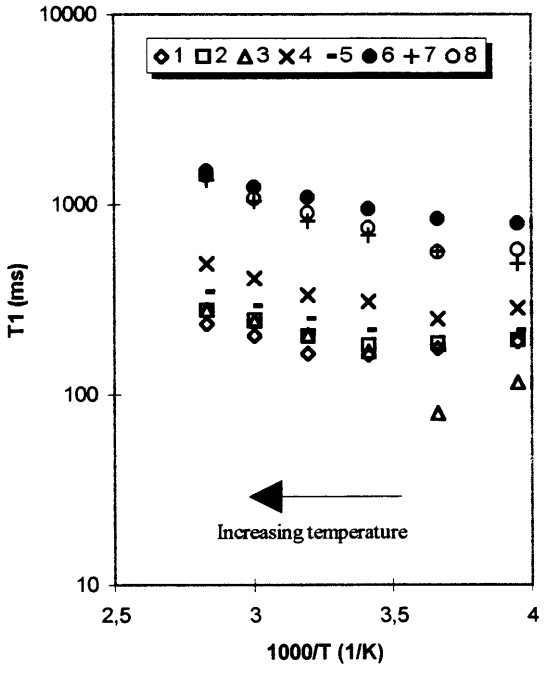

Figure 7. Temperature dependence of the ^{13}C T_1 relaxation times associated with each peak of the ^{13}C CP/MAS spectrum for the as-synthesized zeolite. These relaxation times were measured using the Torchia pulse sequence[17] with contact times between 1 and 10 ms.

in the case of bulk TPABr. Indeed, in the temperature range studied and for all the carbons, our T_1 values are between 100 ms and 1.5 s. In contrast, in the case of bulk TPABr and below 378 K (plastic crystal transition), the ^{13}C T_1 values of the C-1 and C-2 carbons are of the order of 30 and 20 s, respectively.[20] Moreover, we observe that above ambient temperature, the T_1 values of every carbon tend to increase with increasing temperature, with the same slope, indicating that the same dynamics affect the entire cation. The activation energy for this motion is $E_a = 16 \pm 2$ kJ mol^{-1}. The mechanism of spin diffusion associated with the rapid reorientation of the methyl groups cannot account for such a common behaviour for all the different carbons. This is confirmed by the ^{13}C T_1 values measured at ambient temperature with the standard single pulse inversion–recovery experiment for which spin diffusion is non-existent (148, 195, 283, 963 and 817 ms for peaks 1, 2, 3 + 4 + 5, 6 and 7 + 8, respectively). Hence, even the slope for the C-3 carbons is related to a rapid motion that is not the methyl group reorientation. This indicates that an entire cation oscillation is superimposed on the rapid reorientation of the methyl groups and on the reorientational motion which is responsible for the low value of the proton second moment in this temperature domain (Part 1[9]).

CONCLUSION

Recently, Lewis *et al.*[24] carried out a molecular simulation study of the associated TPA-MFI. They showed that a major contribution to the stabilization of the structure was brought by intermolecular interactions within the framework. Among tetramethyl-, tetraethyl-, tetrapropyl- and tetrabutylammonium cations, the tetrapropylammonium cation led to the lowest stabilizing energy of the association. However, different workers have shown that the distance between two intersections in a ZSM-5 zeolite is shorter than the length of two propyl arms.[25,26] Both arguments agree with our high-resolution ^{13}C NMR experiments. Indeed, the indirect proton dipolar coupling measurements, at ambient temperature, have given evidence for the molecular packing effect on the methyl groups resulting in a residual proton dipolar coupling at these carbons. These measurements also showed that each C-1 and C-2 carbon undergoes a motion with increasing amplitude from carbons C-1 to C-2. Moreover, ^{13}C T_1 measurements showed that the entire cation exhibits a superimposed oscillation motion. All these observations emphasize the importance of an inter-cation dynamic equilibrium to satisfy the lowest energy state required for the crystallization process of such a guest–host association. Furthermore, the particularity of the dynamics of the TPA cation during the crystallization process is revealed by the high-temperature ^{13}C CP/MAS spectra. They indicate the appearance of an additional splitting of the low-frequency peak of the C-1

carbon signals. This can be related to the high-temperature decrease of ^1H $T_{1\rho}$ observed in Part 1,[9] which is centered around 440 K (synthesis temperature of the sample). Hence this high-resolution ^{13}C NMR study of the dynamics of the TPA cation appeared to be an interesting complementary approach to the previous ^1H broad-line NMR study. Unfortunately, the detailed nature of these motions could not be identified, probably owing to the inequivalency of the four propyl arms.

Acknowledgements

The authors thank A. C. Faust for providing the sample, Dr H. Forster (Bruker Analytishe Messtechnik, Silberstreifen Rheinstetten) for recording high-temperature spectra and the CRAMPS spectrum and Dr J. Hirschinger (Université Louis Pasteur, Strasbourg) for fruitful discussions. R. G. also thanks Professor Robin K. Harris for helpful discussions.

REFERENCES

1. R. M. Barrer and P. J. Denny, *J. Chem. Soc.* 971 (1961).
2. W. M. Meier and D. H. Olson, *Atlas of Zeolite Structure Types*, 3rd ed. Butterworth-Heinmann, London (1992).
3. R. J. Argauer and G. R. Landolt, *US Pat.* 3 702 886 (1972).
4. R. Szostak, *Handbook of Molecular Sieves.* Van Nostrand Reinhold, New York (1992).
5. H. Gies, in *Advances Zeolite Science and Applications*, edited by J. C. Jansen, M. Stöcker, H. G. Karge and J. Weitkamp, Studies in Surface Science and Catalysis, Vol. 85, p. 295. Elsevier, Amsterdam (1994).
6. S. Hayashi, K. Suzuki and K. Hayamizu, *J. Chem. Soc., Faraday Trans.* **85**, 2973 (1985).
7. C. J. J. den Ouden, K. P. Datema, F. Viesser, M. McKay and M. F. M. Post, *Zeolites* **11**, 418 (1991).
8. K. D. Schmitt and G. J. Kennedy, *Zeolites* **14**, 638 (1994).
9. R. Gougeon, J. M. Chezeau and B. Meurer, *Solid State Nucl. Magn. Reson.* **4**, 281 (1995).
10. F. Lauprêtre, *NMR Basic Principles and Progress*, Vol. 30, p. 63. Springer, Berlin (1994).
11. F. G. Ridell, S. Arumugam, K. D. M. Harris, M. Rogerson and J. H. Strange, *J. Am. Chem. Soc.* **115**, 1881 (1993).
12. J. M. Twyman and C. M. Dobson, *J. Chem. Soc., Chem. Commun.* 786 (1988).
13. K. Zemke, K. Schmidt-Rohr, J. H. Magill, H. Sillescu and H. W. Spiess, *Mol. Phys.* **80**, 1317 (1993).
14. F. Imashiro, D. Kuwahara, T. Nakai and T. Terao, *J. Chem. Phys.* **90**, 3356 (1989).
15. P. Tekely, D. Nicole, J. Brondeau and J. J. Delpuech, *J. Phys. Chem.* **90**, 5608 (1986).
16. P. Palmas, P. Tekely and D. Canet, *Solid State Nucl. Magn. Reson.* **4**, 105 (1995).
17. D. A. Torchia, *J. Magn. Reson.* **30**, 613 (1978).
18. J. M. Chezeau, L. Delmotte, T. Hasebe and N. B. Chanh, *Zeolites* **11**, 729 (1992).
19. J. G. Hexem, M. H. Frey and S. J. Opella, *J. Am. Chem. Soc.* **103**, 24 (1981).
20. J. Cheng, A. Xenopoulos and B. Wunderlich, *Mol. Cryst. Liq. Cryst.* **220**, 105 (1992).
21. J. M. Chezeau, L. Delmotte, J. L. Guth and M. Soulard, *Zeolites* **9**, 78 (1989).
22. J. Virlet, *J. Chim. Phys.* **89**, 359 (1992).
23. G. E. Pake, *J. Chem. Phys.* **16**, 327 (1948).
24. D. W. Lewis, C. M. Freeman and C. R. A. Catlow, *J. Phys. Chem.* **99**, 11194 (1995).
25. J. B. Nagy, Z. Gabelica and E. G. Derouane, *Zeolites* **3**, 43 (1983).
26. K. J. Chao, J. C. Lin, Y. Wang and G. H. Lee, *Zeolites* **6**, 35 (1986).